

A comparative study of alternative methods to determine the response of poly-ethylene terephthalate nuclear track detector

R. Bhattacharyya^{a,*}, S. Dey^a, Sanjay K. Ghosh^{a,b}, Akhil Jhingan^c, A. Maulik^a, L. Patrizii^d, Sibaji Raha^{a,b}, D. Syam^a, V. Togo^d

^aCentre for Astroparticle Physics and Space Science, Bose Institute, Kolkata 700 091, India

^bDepartment of Physics, Bose Institute, Kolkata 700 009, India

^cInter University Accelerator Centre, Aruna Asaf Ali Marg, New Delhi 110067, India

^dINFN, Sezione di Bologna, Viale C. Berti Pichat 6/2, I-40127 Bologna, Italy

Abstract

Two widely used methods of determining the etch-rate ratio in poly-ethylene terephthalate (PET) nuclear track detector are compared. Their application in different regimes of ion's energy loss is investigated. A new calibration curve for PET is also presented.

Keywords: Nuclear Track Detector, Poly-ethylene Terephthalate, Restricted Energy Loss

1. Introduction

Nuclear track detectors (NTDs) find wide use in charged particle detection [1, 2]. They are particularly suited in the search for rare, highly ionizing particles against a large background from low ionizing particles [3, 4, 5, 6, 7, 8].

A charged particle losing energy while passing through an NTD, can create a permanent trail ("latent track") of damaged bonds along its path [1]. On being treated with suitable reagents (chemical etching), if the material along the damage trail is etched out at a faster rate (the track etch-rate, V_T) than the etch-rate of the undamaged material (the bulk etch-rate, V_B), a conical

*Corresponding author

Email address: rupamoy@gmail.com (R. Bhattacharyya)

etch-pit is formed. In nuclear track detectors the size and shape of etch-pits depend on the particle's energy loss - more precisely on the restricted energy loss (REL) - along its path and on its angle of incidence [9, 10]. The minimum REL allowing the formation of an etch-pit, i.e. such that $V_T > V_B$, sets the detector threshold. For a particle impinging perpendicularly to the detector surface, if its energy loss is above threshold and constant, the etch-pit has the shape of a right circular cone. The process is similar to the Mach cone produced by an object moving in a medium at constant supersonic velocity. V_T and V_B play the role of the velocity of the object and that of the sound in the medium, respectively. We can identify the angle α (Fig. 1a) with the Mach angle and $\sin \alpha = V_B/V_T$. The shape of the etch-pit will not be a right-circular cone (or obliquely cut right-circular cone in case of angular incidence) if dE/dx (as well as REL) varies along the latent track. The steepness of the etch-pit's wall increases (Fig. 1b) until the energy loss reaches the Bragg peak [1]. Thus the etch-pit will look like a flared cone [11] as sketched in Fig. 1b.

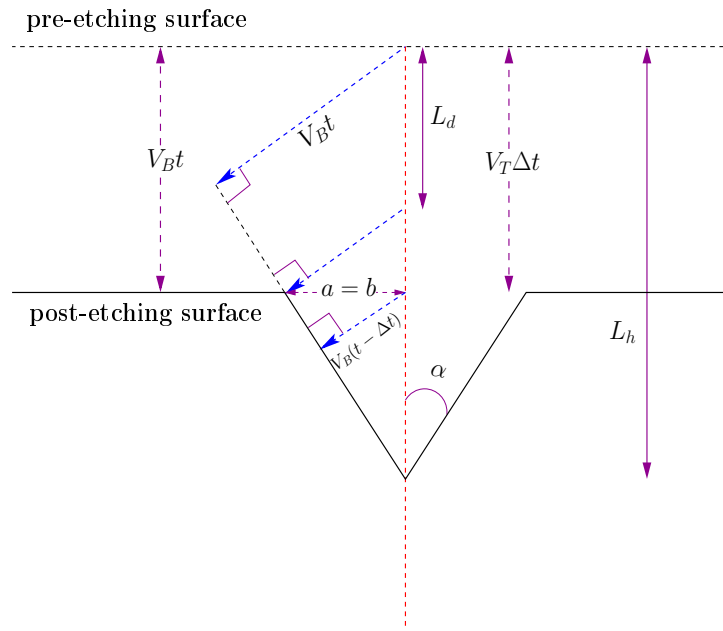
The aim of this paper is to determine the etch-rate ratio of poly-ethylene terephthalate (PET) for ions with energy in the range 0.7 – 11.1 MeV/nucleon.

2. Methods to determine the etch-rate ratio

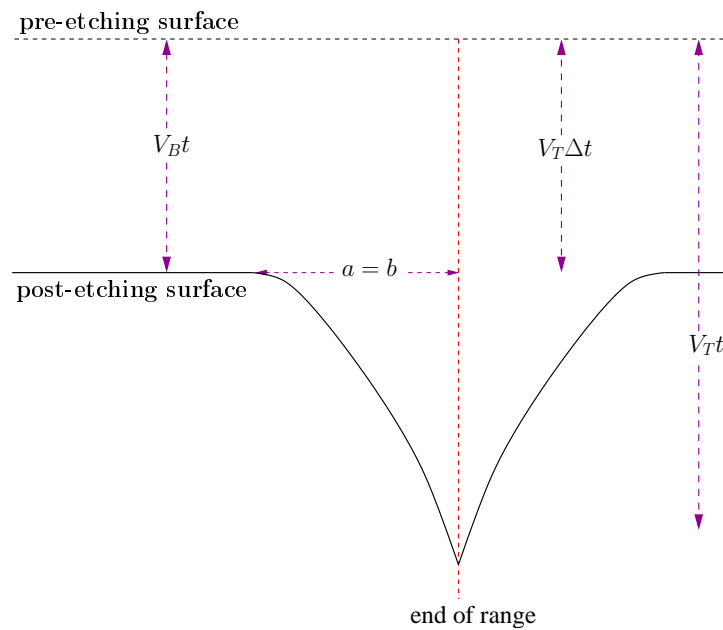
Different methods can be used to calculate the etch-rate ratio $V = V_T/V_B$ from the dimensions of the etch-pits. In this paper, two such methods are compared, which, in general, relate to different regimes of the ion's energy loss. By one method [12] V_T is calculated by measuring the length L_h (Fig. 1a) of the etched out section of the latent track and the etching time (t). The bulk etch-rate V_B is determined by the change in the thickness of the detector sheet over the etching time. With reference to Fig. 2a, for a particle impinging at an angle i with respect to the normal to the detector surface, one has

$$\frac{V_T}{V_B} = \frac{d + V_B t}{V_B t \cos i} \quad (i < \alpha); \quad \frac{V_T}{V_B} = \frac{\mu d' + V_B t}{V_B t \cos i} \quad (i > \alpha) \quad (1)$$

where d (or d') is the vertical distance between the post-etching surface and the tip of the etch-pit cone, as measured by the microscope. The refractive index



(a)



(b)

Figure 1: Sketch of an etch-pit along the latent track of an ion incident normally to the NTD's surface. The energy loss is (a) constant, (b) increasing along the ion's trajectory. Here Δt is the etching time at which the etchant reaches the level of the post-etch surface along the track.

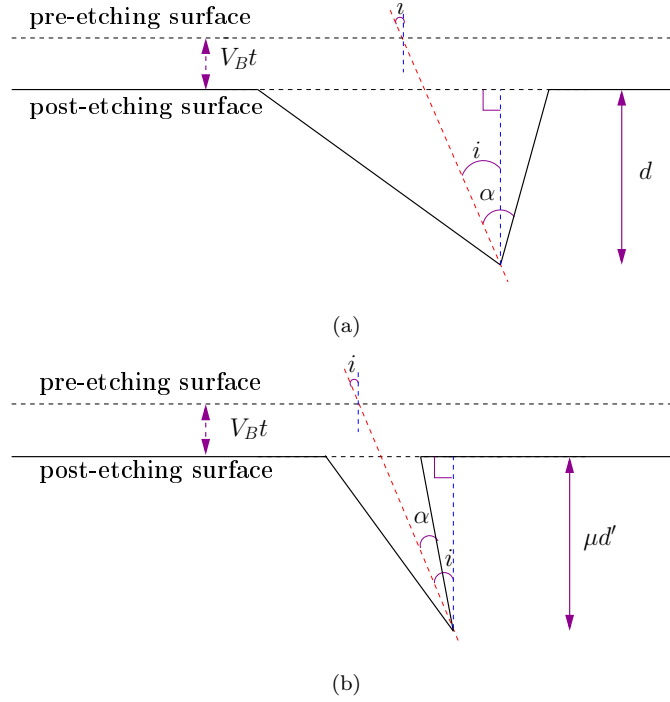


Figure 2: Etched latent track when the ion impinges on the NTD's surface at an angle (a) $i < \alpha$ and (b) $i > \alpha$.

of the detector material, μ , has to be taken into account for $i > \alpha$ (Fig. 2b). The refractive index of PET is $\mu_{PET} = 1.64 \pm 0.02$ in yellow light. It was determined following the same procedure as in [13] and it is identical to the value given in [14]. Henceforth this method of determining V_T/V_B is referred to as “depth measurement method”.

By another method, the average V_T/V_B can be determined from the size of the surface etch-pit opening [15, 16], using Eq. (2)

$$\frac{V_T}{V_B} = \sqrt{1 + \frac{4A^2}{(1 - B^2)^2}} \quad (2)$$

where $A = \frac{a}{V_B t}$ and $B = \frac{b}{V_B t}$; a and b are the semi-major and the semi-minor axis of the elliptical opening of the etch-pit, respectively. For a homogeneous and isotropic material, $B \leq 1$. For a particle impinging normally to the detector surface, the opening of the etch-pit is circular, and $a = b$. This method is

referred to in the following as “diameter measurement method”.

It has to be noted that Eq. (2) provides the average of V_T/V_B over the length $L_d = V_B t V / (V + 1)$ [10] from the pre-etching surface (Fig. 1a), whereas with Eq. (1) the average is over the length $L_h = (d + V_B t) / \cos i$ or $L_h = (\mu d' + V_B t) / \cos i$. Therefore for a slowing down electrically charged particle, the etch-rate ratio computed using Eq. (1) yields a value larger than the one computed using Eq. (2), since V_T/V_B is an increasing function of REL [1, 13, 17].

3. Determination of REL

At the energies of ions used in this paper, the restricted energy loss for NTDs can be computed using Eq. (3) [1]

$$\left(\frac{dE}{dx}\right)_{E < E_{cut}} = C_1 \left(\frac{z^*}{\beta}\right)^2 \left[\ln \left(\frac{W_{max} E_{cut}}{I^2} \right) - \beta^2 - \delta \right] \quad (3)$$

where $C_1 = 2\pi n_e e^4 / m_e^2$; n_e is the number density of electrons in the detector; m_e is the electron mass; z^* is the effective charge of the incoming particle [1]

$$z^* = z [1 - e^{(-130\beta/z^{2/3})}] \quad (4)$$

z and β being the particle’s electric charge and velocity in units of electron charge e and speed of light c , respectively; $W_{max} = 2m_e c^2 \beta^2 \gamma^2$ in the “low-energy” approximation [18] is the maximum energy that can be transferred to an electron in a single collision; γ is the Lorentz factor; δ is the density-effect correction term due to the polarization of the medium, relevant at relativistic energies; I is the material mean ionization potential ($I = 73.2$ eV for PET [19]); E_{cut} is the maximum energy of delta-rays contributing to the formation of the latent track. Hereinafter, $E_{cut} = 350$ eV is assumed to compute REL in polyethylene terephthalate. For calculating the average of REL along the ion’s trajectory, the Monte Carlo code SRIM [20] was used.

4. Experimental method

In order to compare the “depth measurement method” to the “diameter measurement method” when $B \approx 1$, we used 3.8 MeV/A $^{35}\text{Cl}^{10+}$ beam from

the pelletron accelerator and the General Purpose Scattering Chamber at the Inter-University Accelerator Center (IUAC), New Delhi. Details of the beam are given in Table 1. Small pieces ($5\text{ cm} \times 5\text{ cm}$) of $90\text{ }\mu\text{m}$ thick PET films (Desmat Co., India), were mounted on the aluminum holders and placed on the two arms inside the scattering chamber (Fig. 3). PET films were irradiated by $^{35}\text{Cl}^{10+}$ ions backscattered from a gold foil target $250\text{ }\mu\text{g cm}^{-2}$ thick. Exposure

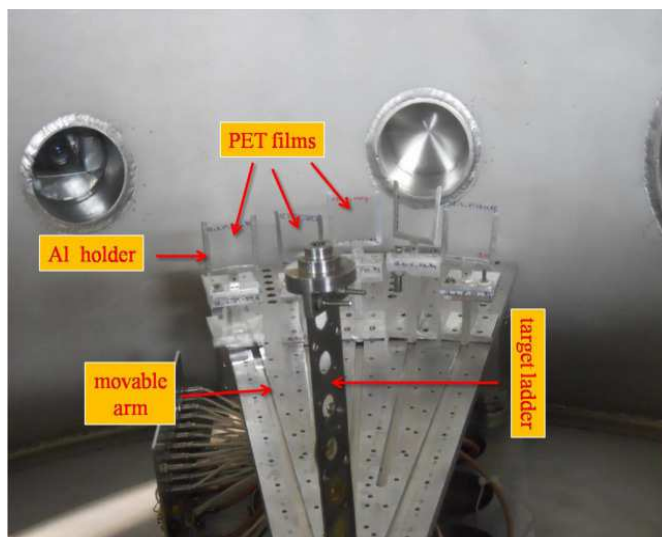


Figure 3: Interiors of the General Purpose Scattering Chamber (diameter 1 m).

duration was controlled such that the ion density on the detector never exceeded $\sim 10^4/\text{cm}^2$ to prevent detector “burnout”. After the exposure, the detectors were etched in a tank (Julabo, Germany) equipped with a motorized stirrer, in 6.25 N NaOH aqueous solution at $55.0 \pm 0.1^\circ\text{C}$ for 3 hours. After etching, the detectors were observed under a Leica DM4000 B optical microscope with a $100\times$ objective and $10\times$ eyepieces. The image analysis software QWin was used for the measurement of etch-pits’ sizes.

5. Results

Data obtained from previous exposures of PET films and from the exposure to $^{35}\text{Cl}^{10+}$ ions are summarized in Table 2 and Table 3. As shown in the last

Ion	Energy per nucleus (MeV)	Beam current (nA)	Charge state
^{35}Cl	132	15	10

Table 1: Properties of the $^{35}\text{Cl}^{10+}$ beam. Beam energy has an uncertainty $< 5\%$.

two rows of Table 3 the values of V_T/V_B for $^{35}\text{Cl}^{10+}$ ions of 70 MeV/nucleus and 77 MeV/nucleus, determined using Eq. (2) are significantly different, although the corresponding values of REL are very close. This happens because of the $(1 - B^2)$ term in the denominator of Eq. (2), when $B \sim 1$ (columns 6 of table 3 and Fig. 4).

Ion	Energy per nucleon (MeV/A)	Incidence angle	Time of etching (hours)	Depth measurement (μm)	Major-axis (μm)	Minor-axis (μm)
$^{32}\text{S}^{9+}$	2.1	0°	1.8	6.53 ± 0.30	2.87 ± 0.15	2.75 ± 0.14
	3.4	0°	2.0	5.32 ± 0.29	2.91 ± 0.14	2.86 ± 0.14
$^{16}\text{O}^{7+}$	1.0	0°	3.0	5.11 ± 0.29	3.62 ± 0.15	3.34 ± 0.15
	1.2	0°	3.0	4.05 ± 0.30	3.54 ± 0.16	3.21 ± 0.16
$^{12}\text{C}^{4+}$	0.7	25°	4.0	5.12 ± 0.29	4.50 ± 0.14	4.09 ± 0.14
	0.9	25°	4.0	4.03 ± 0.29	3.46 ± 0.14	2.76 ± 0.15
$^{35}\text{Cl}^{10+}$	2.0	0°	3.0	12.25 ± 0.29	5.94 ± 0.15	5.87 ± 0.15
	2.2	0°	3.0	10.81 ± 0.29	5.29 ± 0.14	5.26 ± 0.14

Table 2: Data used to compute V_T/V_B using Eq. (1) and Eq. (2). Ions' energies and angles of incidences have an uncertainty $< 10\%$ and $< 4\%$, respectively. Errors in column 5, 6 and 7 include statistical and systematic uncertainties.

It should be mentioned here that there exist innovative ways of increasing the sensitivity of B as the so-called “two-step etching” process [22]. However this method is inapplicable here due to a comparatively shorter range of the incoming particles. As shown in Fig. 4 the normalized semi minor-axis B levels out to ≈ 1 at $REL > 17 \text{ MeV/mg cm}^{-2}$ (similar to what observed in CR-39 at $REL \sim 6 \text{ MeV/mg cm}^{-2}$ [23]). Such reduced sensitivity of the etch-pit diameter (or minor-axis) at large REL s [13] along with systematic uncertainties on a , b and V_B compels one to switch to the depth measurement method for V_T/V_B determination.

Ion	Incident energy per nucleus (MeV)	Energy at the Bragg peak (MeV)	Average REL over the length L_d (MeV/mg cm ⁻²)	Average REL over the length L_h (MeV/mg cm ⁻²)	Normalized semi minor-axis B	V_T/V_B by depth measurement method	V_T/V_B by diameter measurement method
³² S ⁹⁺	67	22.5	14.63 ± 0.22	15.2 ± 1.0	0.75 ± 0.13	4.5 ± 0.7	3.8 ± 1.3
	110		11.86 ± 0.13	12.1 ± 0.4	0.72 ± 0.12	3.7 ± 0.6	3.2 ± 0.9
¹⁶ O ⁷⁺	16	7.0	7.34 ± 0.25	7.8 ± 0.7	0.55 ± 0.12	2.7 ± 0.4	2.0 ± 0.5
	20		6.67 ± 0.15	7.0 ± 0.4	0.53 ± 0.11	2.3 ± 0.4	1.9 ± 0.4
¹² C ⁴⁺	8	5.0	5.9 ± 0.5	6.0 ± 0.4	0.51 ± 0.07	2.1 ± 0.5	1.84 ± 0.25
	11		5.10 ± 0.33	5.5 ± 0.7	0.34 ± 0.07	1.8 ± 0.5	1.40 ± 0.12
³⁵ Cl ¹⁰⁺	70	27.5	–	17.5 ± 2.1	0.97 ± 0.09	5.1 ± 0.5	57 ± 63
	77		–	17.1 ± 2.4	0.88 ± 0.08	4.6 ± 0.4	8 ± 5

Table 3: Data for the different ions incident on PET. Errors on REL are the standard deviation of values computed along the latent track. In column 6, the mean value of the semi-minor axis (b), normalized to the bulk etch length ($V_B t$) [21] is given. In column 7 and 8 are the etch-rate ratios measured by the methods discussed in the text. Errors in column 6, 7 and 8 include statistical and systematic uncertainties.

Calibration of PET nuclear track detector

In previous calibration campaigns, PET films had been irradiated with ²³⁸U, ¹²⁹Xe, ⁷⁸Kr, ⁴⁹Ti beams at REX-ISOLDE CERN [17]; ⁵⁶Fe, ³²S, ¹⁶O beams at IUAC [24]; ¹²C beam at IOP [25]. In Fig. 5, the reduced etch-rate $S = V - 1$, is plotted against REL for data listed in Table 3 and data obtained from previous exposures. On the horizontal axis REL values are the average over the length L_d or L_h for V_T/V_B determined from the depth measurement and the diameter measurement, respectively. Data are fit to a second-degree polynomial equation $S = p_0 + p_1 (REL) + p_2 (REL)^2$, where $p_0 = -(1.15 \pm 0.09)$, $p_1 = 0.331 \pm 0.014$ [MeV/mg cm⁻²]⁻¹ and $p_2 = -(19.2 \pm 2.1) \times 10^{-4}$ [MeV/mg cm⁻²]⁻². The fit adjusted R^2 is 0.987. The detection threshold is at $REL \approx 3.5$ MeV/mg cm⁻² determined by extrapolating the curve to $S = 0$. Therefore PET is able to record particles with $Z/\beta > 125$.

6. Conclusion and discussion

There is one clear advantage of determining V_T/V_B from the diameter measurement method (Eq. (2)) over the depth measurement method (Eq. (1)). In the first case, it is relatively easier to focus the microscope on the opening of the

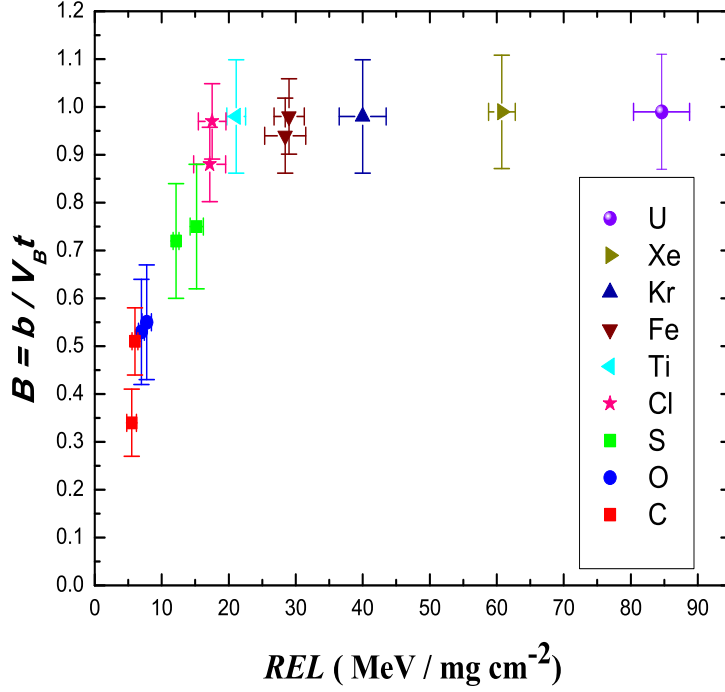


Figure 4: Normalized semi minor-axis B vs. REL plot for different ions, listed in table 3.

etch-pit only, thus reducing effectively the time for large area scanning, compared to depth measurement. However, as we have shown, the diameter measurement method becomes less sensitive for PET NTD detector when $REL \gtrsim 15$ MeV/mg cm⁻². Depth measurement provides higher resolution at larger REL values. In conclusion in identifying a particle using nuclear track detectors, depth measurement method for determining V_T/V_B should be adopted if normalized semi minor-axis $B \approx 1$.

Acknowledgements

We sincerely thank the staffs at the Inter-University Accelerator Center (IUAC), New Delhi, India, especially Mr. N. Saneesh and Mr. Mohit Ku-

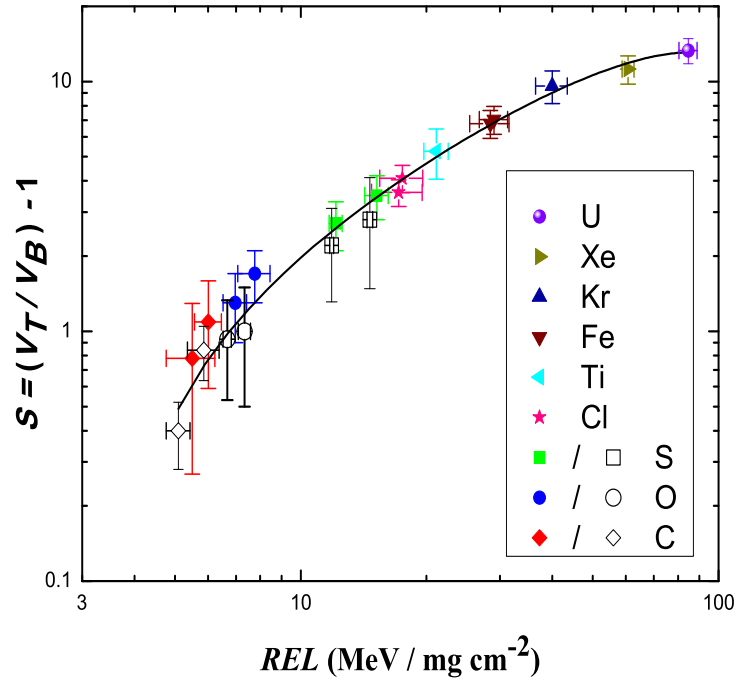


Figure 5: Reduced etch-rate data versus REL for PET using etch-pit depth measurements (filled symbols) and diameter measurements (empty symbols). The curve is the result of the fit to a second order polynomial. The adjusted R^2 value is 0.987.

marfor, for providing all possible support during the chlorine beam exposure. The authors also thank Mr. Sujit K. Basu for technical assistance. The work is funded by IRHPA (Intensification of Research in High Priority Areas) Project (IR/S2/PF-01/2011 dated 26.06.2012) of the Science and Engineering Research Council (SERC), DST, Government of India, New Delhi. LP and VT wish to thank their colleagues at INFN Bologna.

References

- [1] R. L. Fleischer, P. B. Price, R. M. Walker, Nuclear Tracks in Solids. Principles and Applications, University of California Press, Berkeley, 1975.
- [2] S. A. Durrani, R. K. Bull, Solid State Nuclear Track Detection. Principles, Methods and Applications, Pergamon Press, Oxford, 1987.
- [3] S. Balestra, S. Cecchini, M. Cozzi, M. Errico, F. Fabbri, G. Giacomelli, R. Giacomelli, M. Giorgini, A. Kumar, S. Manzoor, J. McDonald, G. Mandrioli, S. Marcellini, A. Margiotta, E. Medinaceli, L. Patrizzii, J. Pinfold, V. Popa, I. E. Qureshi, O. Saavedra, Z. Sahnoun, G. Sirri, M. Spurio, V. Togo, A. Velarde, A. Zanini, Magnetic Monopole search at high altitude with the SLIM experiment, *Eur. Phys. J. C*55 (2008) 57–63. [arXiv:0801.4913](#), [doi:10.1140/epjc/s10052-008-0597-3](#).
- [4] S. Cecchini, M. Cozzi, D. Di Ferdinando, M. Errico, F. Fabbri, G. Giacomelli, R. Giacomelli, M. Giorgini, A. Kumar, J. McDonald, G. Mandrioli, S. Manzoor, A. Margiotta, E. Medinaceli, L. Patrizzii, J. Pinfold, V. Popa, I. E. Qureshi, O. Saavedra, Z. Sahnoun, G. Sirri, M. Spurio, V. Togo, C. Valieri, A. Velarde, A. Zanini, Results of the search for Strange Quark Matter and Q-balls with the SLIM Experiment, *Eur. Phys. J. C*57 (2008) 525–533. [arXiv:0805.1797](#), [doi:10.1140/epjc/s10052-008-0747-7](#).
- [5] S. Cecchini, T. Chiarusi, G. Giacomelli, E. Medinaceli, L. Patrizzii, G. Sirri, V. Togo, Measurement of Cosmic Ray elemental composition from the CAKE balloon experiment, *Adv. Space Res.* 46 (2010) 1382. [arXiv:0911.3500](#), [doi:10.1016/j.asr.2010.07.023](#).
- [6] B. Acharya, J. Alexandre, J. Bernabu, M. Campbell, S. Cecchini, J. Chwastowski, M. De Montigny, D. Derendarz, A. De Roeck, J. R. Ellis, M. Fairbairn, D. Felea, M. Frank, D. Frekers, C. Garcia, G. Giacomelli, M. Giorgini, D. Haegan, T. Hott, J. Jakbek, A. Katre, D. W. Kim, M. G. L. King, K. Kinoshita, D. Lacarrere, S. C. Lee, C. Leroy,

- A. Margiotta, N. Mauri, N. E. Mavromatos, P. Mermoud, V. A. Mitsou, R. Orava, L. Pasqualini, L. Patrizii, G. E. Pvlá, J. L. Pinfold, M. Platkev, V. Popa, M. Pozzato, S. Pospisil, A. Rajantie, Z. Sahnoun, M. Sakellariadou, S. Sarkar, G. Semenoff, G. Sirri, K. Sliwa, R. Soluk, M. Spurio, Y. N. Srivastava, R. Staszewski, J. Swain, M. Tenti, V. Togo, M. Trzebinski, J. A. Tuszyski, V. Vento, O. Vives, Z. Vykydal, A. Widom, J. H. Yoon, The physics programme of the MoEDAL experiment at the LHC, *Int. J. Mod. Phys. A*29 (2014) 1430050. [arXiv:1405.7662](https://arxiv.org/abs/1405.7662), [doi:10.1142/S0217751X14300506](https://doi.org/10.1142/S0217751X14300506).
- [7] S. Banerjee, S. K. Ghosh, S. Raha, D. Syam, Can cosmic strangelets reach the earth?, *Phys. Rev. Lett.* 85 (2000) 1384–1387. [doi:10.1103/PhysRevLett.85.1384](https://doi.org/10.1103/PhysRevLett.85.1384).
- [8] R. Bhattacharyya, S. Dey, S. K. Ghosh, A. Maulik, S. Raha, D. Syam, Study of radiation background at various high altitude locations in preparation for rare event search in cosmic rays, *Journal of Cosmology and Astroparticle Physics* (04) (2017) 035. [doi:10.1088/1475-7516/2017/04/035](https://doi.org/10.1088/1475-7516/2017/04/035).
- [9] E. Benton, W. Nix, The restricted energy loss criterion for registration of charged particles in plastics, *Nuclear Instruments and Methods* 67 (2) (1969) 343 – 347. [doi:10.1016/0029-554X\(69\)90471-6](https://doi.org/10.1016/0029-554X(69)90471-6).
- [10] P. Baiocchi, S. Cecchini, H. Dekhissi, V. Garutti, G. Giacomelli, G. G. Giani, E. Katsavounidis, G. Iori, L. Patrizii, V. Popa, P. Serra, V. Togo, U. Valdre', E. Vilela, Calibration with relativistic and low velocity ions of a CR39 nuclear track detector, *Radiation Measurements* 25 (1) (1995) 145 – 150, *nuclear Tracks in Solids*. [doi:10.1016/1350-4487\(95\)00057-L](https://doi.org/10.1016/1350-4487(95)00057-L).
- [11] D. Nikezic, K. Yu, Formation and growth of tracks in nuclear track materials, *Materials Science and Engineering: R: Reports* 46 (3) (2004) 51 – 123. [doi:10.1016/j.mser.2004.07.003](https://doi.org/10.1016/j.mser.2004.07.003).

- [12] D. Bhowmik, S. Dey, A. Maulik, S. Raha, S. Saha, S. K. Saha, D. Syam, Characterization and calibration of a SSNTD for heavy-ion detection and strangelet search in cosmic rays, *Nuclear Instruments and Methods in Physics Research Section B: Beam Interactions with Materials and Atoms* 269 (2) (2011) 197 – 201. doi:10.1016/j.nimb.2010.10.028.
- [13] S. Balestra, M. Cozzi, G. Giacomelli, R. Giacomelli, M. Giorgini, A. Kumar, G. Mandrioli, S. Manzoor, A. Margiotta, E. Medinaceli, L. Patrizii, V. Popa, I. E. Qureshi, M. Rana, G. Sirri, M. Spurio, V. Togo, C. Valieri, Bulk etch rate measurements and calibrations of plastic nuclear track detectors, *Nuclear Instruments and Methods in Physics Research Section B: Beam Interactions with Materials and Atoms* 254 (2) (2007) 254 – 258. doi:10.1016/j.nimb.2006.11.056.
- [14] J. Elman, J. Greener, C. Herzinger, B. Johs, Characterization of biaxially-stretched plastic films by generalized ellipsometry, *Thin Solid Films* 313-314 (1998) 814 – 818. doi:10.1016/S0040-6090(97)01001-8.
- [15] G. Somogyi, S. Szalay, Track-diameter kinetics in dielectric track detectors, *Nuclear Instruments and Methods* 109 (2) (1973) 211 – 232. doi:10.1016/0029-554X(73)90265-6.
- [16] J. Pinfold, et al., Technical Design Report of the MoEDAL Experiment, MoEDAL collaboration, 2009.
- [17] S. Dey, D. Gupta, A. Maulik, S. Raha, S. K. Saha, D. Syam, J. Pakarinen, D. Voulot, F. Wenander, Calibration of a solid state nuclear track detector (SSNTD) with high detection threshold to search for rare events in cosmic rays, *Astroparticle Physics* 34 (11) (2011) 805 – 808. doi:10.1016/j.astropartphys.2011.02.005.
- [18] B. Rossi, *High-Energy Particles*, Prentice-Hall Inc., New York, 1952.
- [19] M. F. L’Annunziata, *Handbook of Radioactivity Analysis*, Academic Press, Amsterdam, 2013.

- [20] J. F. Ziegler, M. Ziegler, J. Biersack, SRIM the stopping and range of ions in matter (2010), Nuclear Instruments and Methods in Physics Research Section B: Beam Interactions with Materials and Atoms 268 (11) (2010) 1818 – 1823, 19th International Conference on Ion Beam Analysis. doi:10.1016/j.nimb.2010.02.091.
- [21] T. W. Jeong, P. K. Singh, C. Scullion, H. Ahmed, P. Hadjisolomou, C. Jeon, S. Ter-Avetisyan, CR-39 track detector for multi-MeV ion spectroscopy, Scientific Reports 7 (2152) (2017) 1–8. doi:10.1038/s41598-017-02331-w.
- [22] S. Kodaira, S. Naka, N. Yasuda, H. Kawashima, M. Kurano, S. Ota, Y. Ideguchi, N. Hasebe, K. Ogura, Improvement of charge resolution for high Z/β particles in CR-39 nuclear track detectors by means of two-step etching technique, Nuclear Instruments and Methods in Physics Research Section B: Beam Interactions with Materials and Atoms 274 (2012) 36 – 41. doi:10.1016/j.nimb.2011.11.040.
- [23] G. Giacomelli, M. Giorgini, G. Mandrioli, S. Manzoor, L. Patrizii, V. Popa, P. Serra, V. Togo, E. Vilela, Extended calibration of a CR39 nuclear track detector with 158 A GeV 207Pb ions, Nuclear Instruments and Methods in Physics Research Section A: Accelerators, Spectrometers, Detectors and Associated Equipment 411 (1) (1998) 41 – 45. doi:10.1016/S0168-9002(98)00270-8.
- [24] S. Dey, A. Maulik, S. Raha, S. K. Saha, D. Syam, Particle identification with Polyethylene Terephthalate (PET) detector with high detection threshold, Nuclear Instruments and Methods B336 (2014) 163–166. doi:10.1016/j.nimb.2014.07.006.
- [25] R. Bhattacharyya, S. Dey, S. K. Ghosh, A. Maulik, S. Raha, D. Syam, Determination of the detection threshold for polyethylene terephthalate (PET) nuclear track detector (NTD), Nuclear Instruments and Methods in

Physics Research Section B: Beam Interactions with Materials and Atoms
370 (2016) 63 – 66. doi:10.1016/j.nimb.2016.01.011.